RESEARCH PAPER

An integrated microfluidic device for the high-throughput screening of microalgal cell culture conditions that induce high growth rate and lipid content

Sunwoong Bae · Chul Woong Kim · Jong Seob Choi · Ji-Won Yang · Tae Seok Seo

Abstract This study describes the development of a microfluidic device for the high-throughput screening of culture conditions, such as the optimum sodium acetate concentration for promoting rapid growth and high lipid accumulation of *Chlamydomonas reinhardtii*. An analysis of the microalgal growth on the microfluidic device revealed an optimum sodium acetate concentration of 5.72 g L^{-1}. The lipid content, determined by the 4,4-Difluoro-1,3,5,7-tetramethyl-4-bora-3a,4a-diaza-*s*-indacene (BODIPY® 505/515) staining method, increased with the sodium acetate concentration. The results were found to be statistically reproducible with respect to cell growth and lipid production. Other nutrient conditions, including the nitrogen and phosphorus concentrations, can also be optimized on the same microfluidic platform. The microfluidic device performance results agreed well with the results obtained from the flask-scale experiments, validating that the culture conditions were scalable. Finally, we, for the first time, established a method for the absolute quantification of the microalgal lipid content in the picoliter culture volumes by comparing the on-chip and off-chip data. In conclusion, we successfully demonstrated the high-throughput screening of sodium acetate concentrations that induced high growth rates and high lipid contents in *C. reinhardtii* cells on the microfluidic device.

Sunwoong Bae and Chul Woong Kim contributed equally to this work.

S. Bae · C. W. Kim · J. S. Choi · J.-W. Yang · T. S. Seo (✉)
Department of Chemical and Biomolecular Engineering, KAIST, 291 Daehak-ro, Yuseong-gu, Daejeon 305-701, Republic of Korea
e-mail: seots@kaist.ac.kr

J.-W. Yang (✉)
Advanced Biomass R&D Center, 291 Daehak-ro, Yuseong-gu, Daejeon 305-701, Republic of Korea
e-mail: jwyang@kaist.ac.kr

Introduction

Global warming due to CO_2 emissions and the energy crisis due to fossil fuel depletion have necessitated the search for renewable and sustainable energy sources. Biodiesel has recently garnered huge attention as a renewable energy source because it can replace petrodiesel in vehicles while remaining carbon neutral [1, 2]. Biodiesel can be produced from oil crops, such as palm, coconut, rapeseed, and soybean. However, the generation of biodiesel from oil crops can be accompanied by ethical problems, for example, by promoting food scarcity in favor of energy production, because the large land areas required in producing oil crops tend to displace food crops. In addition, the use of cropland for biofuels can increase greenhouse gases by generating emissions during the implementation of land use changes [3]. Unfortunately, biodiesel feedstocks such as waste cooking oil and animal fat also have significant barriers to their widespread use in that the materials are widely distributed, which makes it difficult to collect the materials in one place for mass processing. Under these circumstances, microalgae are considered to be a promising feedstock for biodiesel production because they have a higher growth rate and lipid content than agricultural crops, they require much less land area than other agriculture-based biodiesel feedstocks, and they do not compete with food crops.

Several technical limitations must be overcome before microalgae may be used as an economically viable biomass feedstock for biodiesel production [4, 5]. The barriers to commercialization include the attenuation of light by dense microalgal cultures, which limits the optimal depth of a photobioreactor. Other barriers include a significant risk of

contamination by invasive species in large-scale ponds, difficulties associated with the consistent large-scale production of biomass under harsh outdoor conditions, and the development of economical microalgal cell harvesting and lipid extraction technologies [5]. Most importantly, microalga should ideally be isolated from the environment or improved on an organismal level through genetic engineering to overcome the previously listed obstacles. The desired individual characteristics of ideal microalga are as follows: (1) high yields may be obtained under high light intensity, (2) the microalgae should have large cells with thin membranes, (3) the algae should be insensitive to high oxygen concentrations, (4) they should be robust, stable, and resistant to infection, (5) the microalgae should display a high growth rate and a high lipid content, (6) the microalgae should form floccules, and (7) they should ideally excrete the lipid outside of the cells [6].

Following the isolation or genetic improvement of ideal microalgae candidates, a screening method for identifying the optimal culture conditions should be developed to maximize cell growth, as well as lipid expression, in the genetically improved microalgal strains. Because even a single microalgal strain can respond uniquely to a given culture condition, it is difficult to optimize and establish culture condition libraries through labor-intensive and routine flask culture experiments [7–9].

Recent reports have demonstrated the use of microfluidic devices toward the study of bacteria, algae, yeast [10], mammalian cells [11], and cancer cells [12] in picoliter-scale or nanoliter-scale microchambers. Diverse cultivation methods have been developed using microfluidic devices in an effort to identify optimal microbial growth conditions [13–15]. Therefore, microfluidic devices can offer a breakthrough solution for optimizing and screening culture conditions over a diversity of microalgal strains. To this end, the cultivation of microalgae on droplet-based [16–18] or simple chamber-based microfluidic devices [19] has been reported. However, those previous studies have only examined the growth kinetics and physiology of the microalgal species in the microfluidic devices, and this research field, thus, is still in its infancy.

In this study, *Chlamydomonas reinhardtii*, a model eukaryotic green alga, was cultivated to optimize and screen the culture conditions by investigating the microalgal growth characteristics and the lipid accumulation properties in a high-throughput screening microfluidic device. High-throughput screening was achieved using eight concentration gradient-generating microchannels and five identical C-shaped growth chambers on each microchannel, yielding 40 C-shaped growth chambers in total. The *C. reinhardtii* cells were cultured with variation of the sodium acetate concentration, and the fluorescence intensity of the in vivo chlorophyll of *C. reinhardtii* and BODIPY® 505/515-stained cells was monitored for growth and lipid analysis on the microfluidic device in real time. In addition, we compared the cell growth characteristics and lipid content of *C. reinhardtii* on a chip

with those on the flask scale and correlated the fluorescence BODIPY® 505/515 signal on a chip with the absolute amount of the lipid, thereby enabling the prediction of the lipid amount in the flask-scale experiments from the fluorescence BODIPY® 505/515 intensity obtained from the on-chip *C. reinhardtii* cells.

Materials and methods

Device design and fabrication

Conventional soft lithography methods were used to fabricate the microfluidic device (Fig. 1A) [20]. A 5-μm gap between the ceiling glass and the top of the growth chamber was patterned by photolithography to prevent microalgal cells from escaping the growth chamber during the continuous flow of the liquid medium. The fabrication process involved two steps: patterning the gap and fabricating the microchannels and growth chambers. The concentration gradient-generating microchannels were fabricated to provide a sodium acetate concentration gradient.

The gap between the ceiling and the top of the growth chamber was prepared from a 4-in. silicon wafer that had been treated by O_2 plasma to modify the hydrophilic surface. After impurities had been removed under a stream of N_2 gas, a 5-μm thick layer of negative photoresist SU-8 5 (MicroChem, Newton, MA, USA) was spin-coated onto the silicon wafer at 500 rpm for 10 s and then at 1,000 rpm for 30 s. The system was soft-baked at 65 °C for 1 min and then at 95 °C for 1 min to evaporate the negative photoresist solvent. The target structure was obtained by exposing to ultraviolet (UV) light for 10 s (10 mJ cm^{-2} s^{-1}) through a transparency photomask. After UV exposure, the negative photoresist-coated silicon wafer was post-baked at 65 and 95 °C for 1 min each to solidify the desired gap pattern. An SU-8 resist developer (Micro Resist Technology GmbH, Berlin, Germany) was used to produce the desired pattern. We fabricated a total of 40 units of growth chambers consisting of eight microchannels with five identical chambers to obtain statistically reproducible results in a high-throughput manner.

The microchannels used to generate a sodium acetate concentration gradient, as well as the growth chambers, were fabricated according to a similar photolithography procedure. SU-8 25 (MicroChem, Newton, MA, USA) was spin-coated onto the wafer to a thickness of 30 μm at 1,000 rpm for 10 s and then at 2,000 rpm for 30 s. Next, the device was soft-baked at 65 °C for 1 min and at 95 °C for 3 min. After the spin-coating process, the system was exposed to UV light through a transparency photomask having the print pattern of the desired microchannel structure. The device was then post-baked at 65 °C for 3 min and at 95 °C for 7 min. The dimensions of the microchannel were 200 μm in width and 30 μm in height, and

the total volume of the microchannel at the bottom polydimethylsiloxane (PDMS) layer was approximately 260 μL. The mold containing the microchannels and growth chambers was prepared for PDMS casting. PDMS was mixed with the curing agent in a ratio of 1:10. The mixture of PDMS and the curing agent was then poured onto the SU-8 molder, degassed thoroughly for 15 min, and thermally cured at 80 °C in an oven overnight.

The microfluidic device consisted of three layers, including two PDMS layers and one glass layer. The bottom PDMS layer included the gradient-generating microchannels and the cell growth chambers, whereas the top PDMS layer included two inlet holes and one outlet hole, which had been punched manually. The glass layer was entirely rinsed with ethanol to create sterile culture conditions prior to microfluidic device assembly. A stream of N_2 gas was used to remove any liquid residue or impurities from the glass layer and PDMS layer. After exposure to UV light (Ahtech LTS, Seoul, South Korea) for 3 min, the PDMS and glass wafer were assembled and were incubated at 80 °C overnight to improve bond robustness.

Microalgal culture on a chip

Microfluidic channels were modified with bovine serum albumin (Sigma-Aldrich, St. Louis, MO, USA) for 2 h prior to microalgal cell inoculation into the microfluidic device. This step prevented the nonspecific binding of cells onto the microfluidic channel surface. The inlets and outlets of the microfluidic device were connected to a polytetrafluoroethylene (PTFE) tube with an inner diameter of 0.040 in. and an outer diameter of 0.070 in. (Saint-Gobain Performance Plastics Corporation, Akron, OH, USA). All fluids were loaded into the microfluidic device using glass syringes (Hamilton Company, Nevada, USA), and the flow rates were controlled using a syringe pump (KCI Scientific, Seoul, Republic of Korea). Two 5-mL sterile glass syringes (one for the Tris–acetate–phosphate [TAP] medium injection and the other for the sodium acetate injection with a TAP medium) were connected to the two inlets on the microfluidic device through a PTFE tube, while each tube was connected to the 2.5-mL sterile glass syringes in the middle through a low-pressure four-port switching valves (IDEX Health & Science LLC Home of Upchurch Scientific Products, Oak Harbor, WA, USA) to inject the *C. reinhardtii* cells.

C. reinhardtii cells at the early stationary phase were injected with a flow rate of approximately 2 μL min^{-1} to initiate microalgal cell capture. *C. reinhardtii* cells were trapped in each growth chamber due to the size difference between the cell and the intra-chamber gap. The average size of the initially captured *C. reinhardtii* cells was typically 10 μm in diameter. *C. reinhardtii* cells that could not be captured inside the chamber were flushed out through a side port. The culturing solution was infused over 10 min to ensure that a constant baseline of inoculum was introduced to enable a comparative

analysis of *C. reinhardtii* growth in the growth chambers under different culture conditions. The inoculated *C. reinhardtii* were cultivated at a light intensity of 120 μmol photons m^{-2} s^{-1} and were provided with a sodium acetate concentration gradient. Flow injection was switched from the *C. reinhardtii* cell suspension to the TAP medium immediately following the capture of a given amount of *C. reinhardtii* in the growth chamber. The flow rate of the suspension was fixed at 5 μL min^{-1} to overcome the pressure drop across the microchannels. The cell growth rate was evaluated by observing the fluorescence intensities of the chlorophyll of *C. reinhardtii* cells, and lipid expression was quantified by staining the neutral lipids inside the *C. reinhardtii* cells with BODIPY 505/515 (Invitrogen, Carlsbad, CA, USA) solution. The BODIPY® 505/515 infusion procedure was the same as the procedure used to infuse the cell suspension.

The microfluidic device was positioned on a laser scanning confocal microscope (ECLIPSE C1Si, Nikon, Tokyo, Japan) configured to collect time-lapse live cell imaging every 6 h for 18 h, and individual images were characterized using the Nikon EZ-C1 software to evaluate microalgal growth based on the fluorescence intensity of the in vivo chlorophyll in *C. reinhardtii*. The specific growth rate of microalgae in the microfluidic device was calculated using the following equation: $\mu = \ln(I_2/I_1)/(t_2/t_1)$, where μ is the specific growth rate (per hour) and I_1 and I_2 are the relative fluorescence intensities on the microfluidic device at times t_1 and t_2, respectively. After incubation for 42 h, *C. reinhardtii* cells in each growth chamber were stained with the 1-μM BODIBY solution diluted with the TAP medium. The fluorescence intensities of chlorophyll over the whole chamber area were measured at 650 nm in the growth analysis, whereas the fluorescence intensities of *C. reinhardtii* cells stained with BODIPY® 505/515 over the cell-occupied area were measured at 515 nm in the lipid analysis.

Microalgal strain and culture conditions on the flask scale

The microalga *C. reinhardtii* was incubated and subcultured using the TAP agar medium on a regular basis. For the flask-scale experiments, seed cultures of *C. reinhardtii* were prepared in a filter-cap cell culture flask containing 100 mL of the TAP medium. The flasks were shaken at 120 rpm at 25 °C under 120 μmol photons m^{-2} s^{-1}. The light intensity was measured using a light meter (LI-250, LI-COR, Lincoln, NE, USA) equipped with a quantum sensor (LI-190, LI-COR, Lincoln, NE, USA). After incubating for 3 d, the seed cultures were harvested by centrifugation at 7,000 rpm for 5 min and resuspended with a fresh medium. The suspended cells were subsequently added in the appropriate inoculum size to the cell culture flasks containing a 200-mL TAP medium and 0, 1, 2, 5, or 10 g L^{-1} sodium acetate as the organic carbon source. All microalgal cultures were incubated with shaking at 120 rpm and 25 °C under 120 μmol photons m^{-2} s^{-1}.

The optical density of the microalgal culture was measured at 750 nm using a UV–Vis spectrophotometer (DU730, Beckman Coulter, Munich, Germany). The dry cell weight of the microalgal biomass was measured by filtering an aliquot of the algal suspension through a pre-dried and pre-weighed 0.45-μm cellulose nitrate membrane filter (Whatman, Piscataway, NJ, USA). The cells were dried in an oven at 80 °C for 24 h. The correlation between the optical density at 750 nm (OD_{750}) and the dry cell weight for *C. reinhardtii* was found to be described by the following linear regression: $Y=0.7417X+0.0705$ ($R^2=0.9869$), where Y is the cell concentration (in grams per liter) and X is the optical cell density at 750 nm. The specific growth rate of the microalgae in the flasks was calculated using the following equation: $\mu = \ln(C_2/C_1)/(t_2/t_1)$, where μ is the specific growth rate (per hour) and C_1 and C_2 are the cell concentrations at times t_1 and t_2, respectively.

The microalgal cells were harvested by centrifugation at 7,000 rpm for 5 min after cultivation for 3 or 6 d, washed twice with deionized water, dried at 80 °C for 24 h, and ground with a mortar and pestle to facilitate lipid extraction. A certain amount of the ground microalgal biomass was subjected to a lipid extraction step using chloroform/methanol (2:1 *v/v*) according to the Folch method with slight modification. The extracted lipids were subsequently converted to fatty acid methyl esters (FAMEs) by the addition of methanol and sulfuric acid as a catalyst at 100 °C for 10 min. Heptadecanoic acid was used as an internal standard for the fatty acid analysis. After the transesterification reaction, the organic phase containing FAMEs was separated by adding deionized water and then recovered by centrifugation at 4,000 rpm for 10 min. The FAMEs in the organic phase was analyzed by gas chromatography (HP6890, Agilent, Santa Clara, CA, USA) using a flame ionization detector.

Results and discussions

Design of the microfluidic device for microalgal cell cultivation

The microfluidic device for microalgal cell culture was composed of three layers: a PDMS layer, a glass layer, and the patterned PDMS layer from top to bottom. Two inlet holes and one outlet hole were patterned in the top PDMS layer and the glass layer, and the glass wafer was sandwiched between the two PDMS layers in order to prevent any collapse of the PDMS channel and structure during the bonding process. In the bottom patterned PDMS layers (Fig. 1A), we fabricated eight concentration gradient-generating microchannels, and each microchannel contains five C-shaped cell culture chambers. The concentration gradient-generating microchannels function as a passive mixer to produce a serially diluted

solution in parallel. We tested the concentration gradient by adding fluorescein (FAM) solution in the right inlet and water in the left inlet. Gradually intensified fluorescence was observed from the left to right channel, and the increment of the fluorescence signal was linear (Fig. 1B, C). We adapted such concentration gradient-generating microchannels to investigate the effect of the concentration of carbon source, sodium acetate in our case, on the growth rate and lipid expression of *C. reinhardtii* cells. The concentration gradient of the sodium acetate carbon source was generated by injecting the TAP medium solution and a 10.00-g L^{-1} sodium acetate solution individually into the two inlet holes. Ten minutes was required to successfully establish a concentration gradient of sodium acetate on the microchannel ranging from 0.00 to 10.00 g L^{-1}. The resultant concentrations in the microchannels were theoretically 0.00, 1.43, 2.86, 4.29, 5.72, 7.15, 8.58, and 10.00 g L^{-1} from left to right. The flow rates of the two types of solution were fixed at 5 μL min^{-1} after the stream had been stabilized.

Following the concentration gradient-generating microchannels, the C-shaped cell culture chambers were fabricated with five chambers in each microchannel. Figure 1D shows a scanning electron microscope image of an individual microchamber. The cell chamber was designed as 120 μm in diameter and 25 μm in height, and the chamber volume was 904 pL. Since the channel depth was patterned by 30 μm, the gap between the assembled glass wafer and the top of the C-shaped chamber structure was 5 μm (Fig. 1E). Such a gap was narrow enough to capture *C. reinhardtii* whose size was between 9 and 15 μm during the cell-seeding step. The glass wafer was inserted between the two PDMS layers to precisely maintain the narrow gap during the fabrication process. If the top PDMS layer was directly bonded to the bottom patterned PDMS layer, the 5-μm gap could not be uniformly formed due to the elastomeric property of PDMS which resulted in inconsistent concentration gradients and different cell capture yields in each culture chamber. The use of the bottom PDMS layer allows the permeation of gases such as O_2 and CO_2, so that the mixotrophic culture of microalgae is feasible.

Growth analysis on the microfluidic device

Microalgal growth may, in principle, be evaluated from the cell concentrations determined from the dry cell weight or from the chlorophyll content which can be analyzed by solvent extraction methods. However, it is difficult to assess microalgal growth as a function of the cell concentration, cell number, or chlorophyll content on a microfluidic device due to the insufficient quantity of samples. Thus, we utilized the fluorescence intensity measurements of the in vivo chlorophyll in the cells to estimate microalgal growth on a chip.

C. reinhardtii cells were inoculated into each growth chamber with a quite equivalent inoculum size to analyze microalgal growth. The effect of organic carbon source
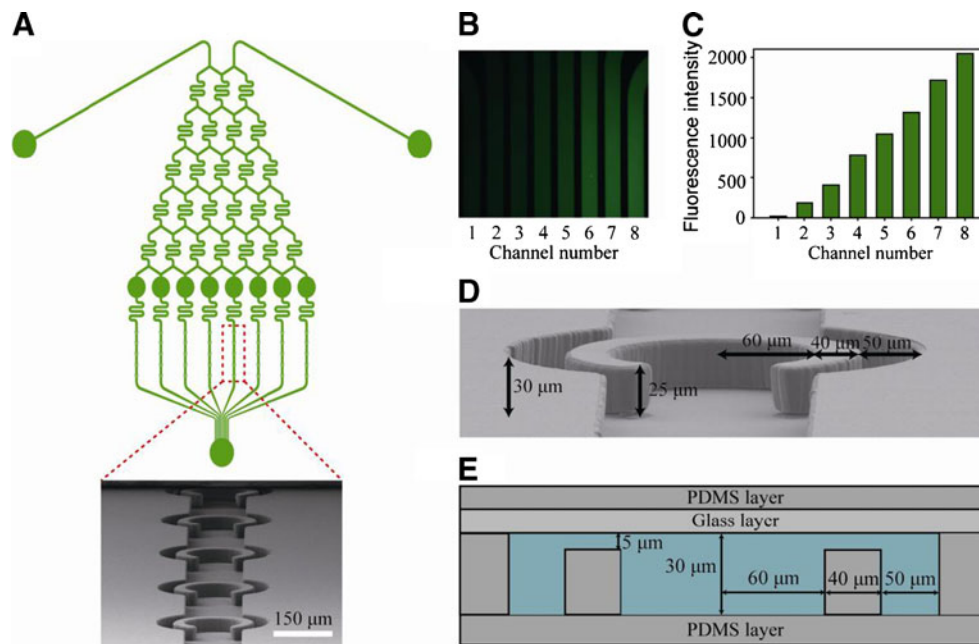
Fig. 1 Illustration of the integrated microfluidic device for high-throughput screening of microalgal cell culture conditions. (A) Schematic diagram showing the integrated microfluidic device which consists of the concentration gradient-generating microchannels and the microalgal culture chambers. (B) Fluorescence image showing the serially diluted FAM concentration from *right* to *left* by the concentration gradient-generating microchannels. (C) Concentration gradient profile by plotting the fluorescence intensity versus the channel position (channel numbers from *1* to *8* are matched with the microchannels from *left* to *right*). (D) A SEM image of the single C-shaped culture chamber unit. (E) Cross-sectional schematics for the assembled microfluidic device

concentration on microalgal growth was investigated by adjusting the sodium acetate concentrations in each microchannel to 0.00, 1.43, 2.86, 4.29, 5.72, 7.15, 8.58, and 10.00 g L^{-1}, respectively, and microalgal cells were incubated for 18 h.

The time-lapse confocal microscopy images showed negligible growth of *C. reinhardtii* at 0.00 and 10.00 g L^{-1} sodium acetate over 18 h, whereas the growth of *C. reinhardtii* at 5.72 g L^{-1} sodium acetate was significant enough to fill the growth chamber with cells (Fig. 2A, left image). Correspondingly, the fluorescence image of the in vivo chlorophyll content, collected every 6 h for 18 h, revealed the same results (Fig. 2A, right image). Figure 2B–E shows the fluorescence intensity profiles of the in vivo chlorophyll content of *C. reinhardtii* cultured under various sodium acetate concentrations over 18 h. Although no significant differences in the fluorescence intensity were observed between each sodium acetate concentration at 0 h (Fig. 2B), the fluorescence intensities at 4.29, 5.72, 7.15, and 8.58 g L^{-1} of sodium acetate increased remarkably after 6 and 12 h incubation (Fig. 2C, D). After 18 h, the fluorescence intensities of the in vivo chlorophyll content at 0.00, 1.43, 2.86, 4.29, 5.72, 7.15, 8.58, and 10.00 g L^{-1} sodium acetate were 158.5, 206.3, 220.4, 476.8, 490.0, 464.4, 447.3, and 184.0, respectively (Fig. 2E). *C. reinhardtii* cells at 4.29, 5.72, 7.15, and 8.58 g L^{-1} sodium acetate took up sufficient quantities of the organic carbon, so their growth increased noticeably. By

contrast, the growth of *C. reinhardtii* cells at 0.00, 1.43, and 2.86 g L^{-1} sodium acetate was relatively slow due to an insufficient supply of organic carbon. The growth rate of *C. reinhardtii* cells was slow at 10.00 g L^{-1} sodium acetate, which was attributed to the inhibitory effects of the high organic carbon concentration [21]. The optimal sodium acetate concentration range for promoting the growth of *C. reinhardtii* was 4.29–8.58 g L^{-1} in the microfluidic system. The addition of 5.72 g L^{-1} sodium acetate enhanced the growth of *C. reinhardtii* by a factor of 3 compared to the growth at 0.00 g L^{-1} sodium acetate [22]. It should be noted that the TAP medium contains a relatively small quantity of acetic acid (1.049 g L^{-1}), which provides an organic carbon source in all cases. All results were analyzed by averaging the values obtained in five identical growth chambers in each microchannel. Thus, we successfully demonstrated the optimization of the sodium acetate concentration for microalgal growth using a microfluidic device within an 18-h incubation period. These results were comparable to the previous reports which were performed on the off-chip basis, demonstrating the proof of principle of high-throughput microalgae culture on the microfluidic device [2]. Although sodium acetate was the only organic carbon source in this high-throughput microalgal culture condition screening system, other nutrients such as nitrogen and phosphorus, which are essential for the photosynthetic growth of microalgae, can be optimized in a similar way.

Fig. 2 Growth analysis of *C. reinhardtii* cells on the microfluidic device. (**A**) Bright-field images of *C. reinhardtii* cultures (*left panel*) and the fluorescence images of the in vivo chlorophyll of *C. reinhardtii* (*right panel*) at 0.00, 5.72, and 10.00 g L^{-1} sodium acetate over the course of 18 h (×600 magnification and 50 μm scale bar). Fluorescence intensity profiles of the in vivo chlorophyll in *C. reinhardtii* cells cultured at various sodium acetate concentrations with incubation times of (**B**) 0 h, (**C**) 6 h, (**D**) 12 h, and (**E**) 18 h
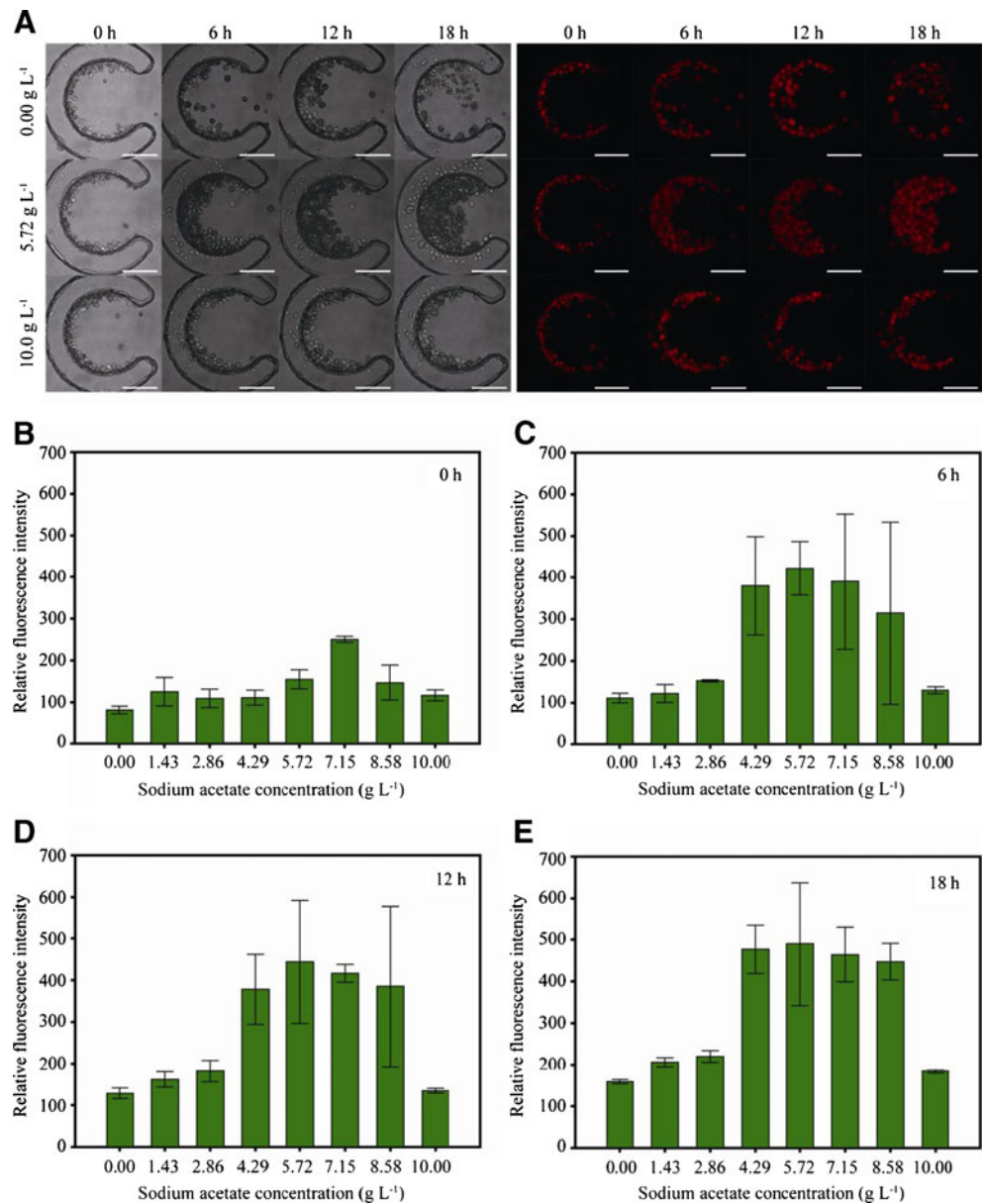
Comparison of the microalgal growth in the microfluidic device and in a flask

Although the microfluidic device offers a valuable tool for microalgal researches by providing a high-throughput analysis platform, it is necessary to set up the correlation between the data produced in a picoliter or nanoliter volume microchamber and the data obtained by a flask scale to make the on-chip data meaningful to the researchers who ordinarily operate the microalgal culture in a flask scale. Thus, we validated the scalability of our technique by comparing the microalgal growth characteristics on the microfluidic device with those obtained from the flask scale.

First, the fluorescence intensity values of the in vivo chlorophyll at each sodium acetate concentration and time were

measured in the cell culture area (diameter of 120 μm) by using a laser scanning confocal microscope and then were normalized relative to the initial intensity value at 0 h to facilitate a comparison (Fig. 3A). The normalized fluorescence intensities of the in vivo chlorophyll at 0.00, 2.86, 5.72, 8.58, and 10.00 g L^{-1} were found to increase by factors of 1.94, 2.01, 3.16, 3.04, and 1.57, respectively, after an 18-h incubation period. The optimum sodium acetate concentration for promoting *C. reinhardtii* growth was confirmed to be 5.72 g L^{-1}. The microalgal growth at 8.58 g L^{-1} was also close to that of 5.72 g L^{-1}. However, *C. reinhardtii* did not grow significantly at 0.00, 2.86, and 10.00 g L^{-1} over the 18-h period due to the improper supply of the organic carbon source.

To compare the on-chip data of Fig. 3A with those produced in a large scale, *C. reinhardtii* cells were cultured at
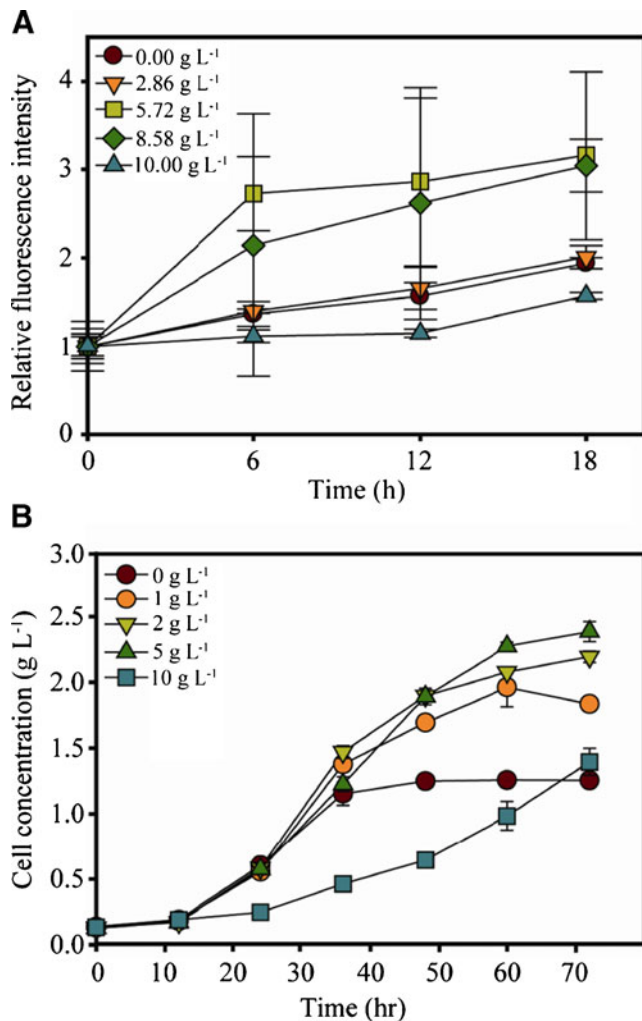
Fig. 3 Comparison of the growth profiles between the microfluidic device and the flask scale. (**A**) Growth curves of *C. reinhardtii* cultured at various sodium acetate concentrations on the microfluidic device. Fluorescence intensity values were normalized to permit a relative quantitative analysis of growth rates. (**B**) Growth curves of *C. reinhardtii* cultured at various sodium acetate concentrations on the flask scale

various sodium acetate concentrations (0, 1, 2, 5, and 10 g L^{-1}) on the flask scale. Microalgal growth curves generally include the lag, exponential, stationary, and death phases in the batch system. The growth characteristics of microalgae, such as the length of the lag phase, the specific growth rate, and the maximum cell concentration, were found to vary with the concentration of the organic carbon source. In the flask-scale cultivation experiments, the inoculum size was fixed at 0.12 g L^{-1} for all sodium acetate concentrations. The elapsed times required to reach the stationary phase at 0, 1, 2, 5, and 10 g L^{-1} sodium acetate were 48, 60, 72, 72, and 132 h, respectively (Figs. 3B and S1 in the Electronic supplementary material). The duration of the stationary phase also differed according to the sodium acetate concentration. Although the duration of the stationary phase at 1, 2, and 10 g L^{-1} was very short, it was relatively long at 0 and 5 g L^{-1}. The maximum

cell concentrations at 0, 1, 2, 5, and 10 g L^{-1} sodium acetate were 1.25, 1.96, 2.19, 2.54, and 2.16 g L^{-1}, respectively. Although the growth rates at all sodium acetate concentrations were nearly identical during the initial 24 h, except at 10 g L^{-1}, the growth rates after 24 h were ordered according to 5>2> 1>0 g L^{-1} sodium acetate. The growth rate at 10 g L^{-1} was lower than the growth rate at the other concentrations due to the excess of organic carbon, although the maximum cell concentration reached 2.16 g L^{-1} after 132 h. As mentioned previously, high organic carbon concentrations introduced inhibitory effects owing to the elevated osmotic pressure.

Table 1 lists the specific growth rates of *C. reinhardtii* when cultured at various sodium acetate concentrations on the microfluidic device and on the flask scale. The specific growth rates of *C. reinhardtii* cultivated at 0.00 g L^{-1} sodium acetate on the microfluidic device and on the flask scale agreed well, although the other sodium acetate concentration conditions displayed slight differences. These results were caused by the difference in the nutrient feeding method. The nutrients were supplied continuously on the microfluidic device, whereas nutrients were supplied in batch mode under the flask-scale cultivation conditions. Despite the absolute value difference between the specific growth rates, the microfluidic device and flask scale displayed the same overall trend in that the optimum sodium acetate concentration, identified based on the growth rate and maximum cell density, was around 5.00 g L^{-1} in both culture systems.

The comparative analysis results indicated that growth on the microfluidic device could be associated with scaling the system to the flask scale. Thus, the optimal sodium acetate culture conditions for promoting microalgal growth on the microfluidic device were successfully screened. The time required for screening the optimal sodium acetate concentrations on a chip was only 18 h, much shorter than the 72 h required on the flask scale.

Lipid analysis

Instead of using a conventional gas chromatography method, lipid analysis on the microfluidic device was performed using the BODIPY® 505/515 staining method. Microalgal cells begin to accumulate lipids in their bodies after reaching the stationary phase [9, 23]. The lipid contents were usually analyzed during the late stationary phase because the lipid content during the exponential or early stationary phase was relatively low. Unfortunately, no differences were observed in the lipid contents of the cells grown under various sodium acetate concentrations after an 18-h incubation period (Fig. 4B). Thus, we incubated the cells for an additional 24 h to accumulate the lipids in the body. After 42 h of incubation, *C. reinhardtii* cells in each growth chamber were stained with BODIPY® 505/515, transmission and fluorescence images were obtained by laser scanning confocal

Table 1 Specific growth rate of *C. reinhardtii* on the microfluidic device and in the flask

	Microfluidic device					Flask scale				
Sodium acetate concentration (g L^{-1})	0.00	2.86	5.72	8.58	10.00	0.00	1.00	2.00	5.00	10.00
Specific growth rate μ (h^{-1})	0.052	0.056	0.167	0.127	0.019	0.054	0.076	0.077	0.064	0.054

microscopy, and then the lipid content was analyzed (Fig. 4A, B). The fluorescence intensities of the BODIPY® 505/515 stained cells at 0.00, 1.43, 2.86, 4.29, 5.72, 7.15, 8.58, and 10.00 g L^{-1} sodium acetate after 42 h incubation were 246.8, 324.3, 348.9, 371.8, 434.8, 447.4, 467.9, and 550.9, respectively, whereas the fluorescence intensity values of the BODIPY® 505/515 stained cells after 18 h were 97.3, 98.1, 76.7, 69.1, 63.0, 68.8, 78.2, and 103.2, respectively. The fluorescence intensity data were obtained from five identical growth chambers on each microchannel. These results indicated that *C. reinhardtii* cells reached the exponential or early stationary phase after 18 h and that the cells could not sufficiently accumulate lipids. After 42 h, the cells reached the middle of the stationary phase, at which point they could accumulate neutral lipids in their bodies. The BODIPY® 505/515 fluorescence intensity became higher in proportion to the sodium acetate concentrations in the microfluidic device.

Higher sodium acetate concentrations can induce *C. reinhardtii* cells to accumulate lipids to a greater degree than that observed at lower sodium acetate concentrations. However, higher sodium acetate concentrations are not always better than lower concentrations in terms of productivity. When evaluating the optimal culture conditions, it is important to consider both the lipid content (in percent, grams lipid per gram cell) and the growth rate (in grams cell per liter per day) because the amount of lipids is directly related to the biomass quantity. In other words, lipid productivity (in grams lipid per liter per day), which is obtained by multiplying the lipid content with the growth rate, must be considered rather than the lipid content itself. A sodium acetate concentration of 5.72 g L^{-1} was the optimum concentration condition on the microfluidic device based on the lipid productivity measurements (Figs. 3A and 4B).

Lipid production on the flask scale was examined for comparison purposes. *C. reinhardtii* cells were cultured at
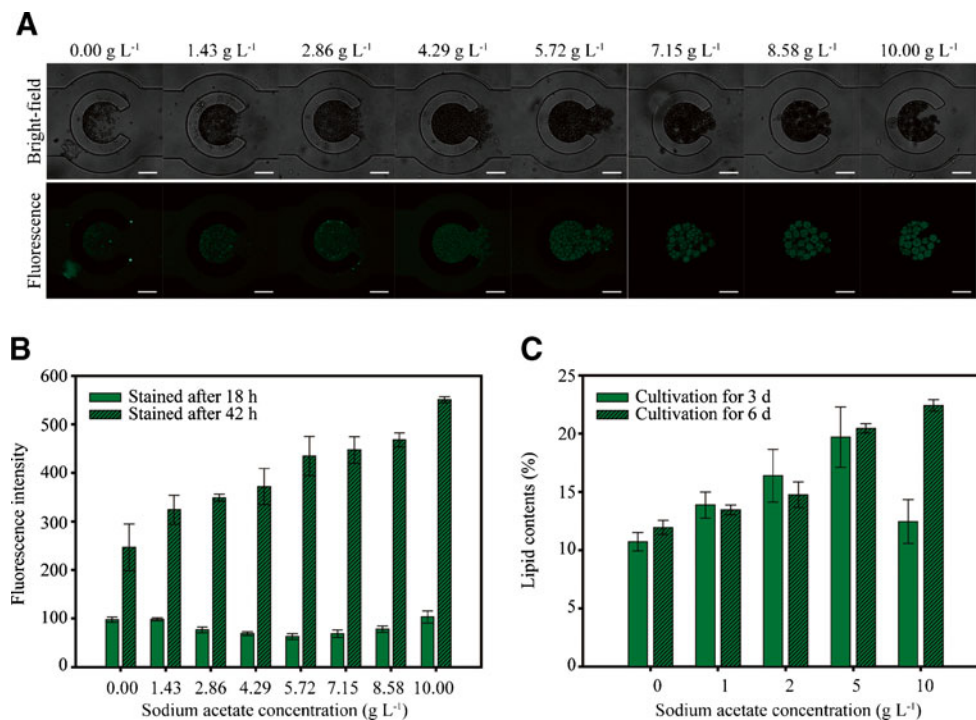

Fig. 4 Lipid analysis of *C. reinhardtii* cultured on the microfluidic device. (**A**) Bright-field images of *C. reinhardtii* cultured for 42 h (*top panel*) and the fluorescence images of *C. reinhardtii* stained with BODIPY® 505/515 (*bottom panel*) for detecting neutral lipids after 42 h cultivation (×400 magnification and 50 µm scale bar). (**B**) Fluorescence intensity of the BODIPY-stained *C. reinhardtii* cells cultured at various sodium acetate concentrations on the microfluidic device. BODIPY staining was performed after 18 and 42 h culture times, respectively. (**C**) Lipid content of *C. reinhardtii* cells cultured at various sodium acetate concentrations on the flask scale. Microalgal cells were harvested after 3 and 6 d cultivation times, respectively. The lipid content was analyzed by gas chromatography

various sodium acetate concentrations on the flask scale, and the cells were harvested after 3 or 6 d. The lipids in the cells were extracted and converted to FAMEs for gas chromatography analysis. The lipid contents in the *C. reinhardtii* cells cultivated at 0, 1, 2, 5, and 10 g L^{-1} sodium acetate for 3 d were 10.7, 13.9, 16.4, 19.7, and 12.4 %, respectively, whereas those for 6 d were 11.9, 13.4, 14.8, 20.4, and 22.4 %, respectively (Fig. 4C). The lipid content of *C. reinhardtii* cells cultivated for 3 d increased proportionally to the sodium acetate concentrations, except at 10 g L^{-1}. The lipid content of *C. reinhardtii* cells cultivated for 3 d at 10 g L^{-1} concentration was lower than the lipid content obtained from the cells cultivated for 6 d because the cells were in the middle of their exponential phase on day 3. The cells had not yet had a chance to synthesize and accumulate the lipids, as shown in Fig. 3B. The lipid content of *C. reinhardtii* cells cultivated for 6 d displayed trends that agreed with the results obtained from the 42-h cultivation in the microfluidic device. We concluded that the high-throughput screening of sodium acetate concentrations, as an organic carbon source that induces a high growth rate and lipid content, was successfully achieved using the microfluidic device. Lipid productivity was quantitated based on fluorescence intensity measurements of the in vivo chlorophyll and neutral lipids stained using BODIPY® 505/515. The parallel flask-scale experiments show cell growth rate and lipid content results similar to the on-chip data with different timescales, demonstrating the validation of scalability.

Absolute quantification of the lipid content on the microfluidic device

Despite the successful development and demonstration of the microfluidic device for the high-throughput screening of sodium acetate concentrations that promote microalgal growth and lipid production, the absolute lipid contents could not be quantified. If the on-chip data can be correlated with the absolute quantity of lipid, it would be very useful for the bioengineers to optimize the cell culture conditions in a large scale to save time, labor, and costs associated with screening. Thus, we correlated the florescence intensity of the BODIPY® 505/515 stained *C. reinhardtii* cells on a chip with the absolute lipid content. The cells cultured in a flask (Fig. 4C) were stained by BODIPY® 505/515 dyes, loaded into the cell chamber on a chip, and then the fluorescence intensities were measured, while the absolute lipid content of the cells were determined by gas chromatography. The relationship could be described by in the following linear expression: $Y = 0.0232X + 5.2876$ ($R^2 = 0.9230$), where Y is the lipid content (in percent) and X is the fluorescence intensity of *C. reinhardtii* cells stained with BODIPY® 505/515 on a chip (Fig. 5). We calculated the actual lipid contents of *C. reinhardtii* after 42 h incubation by using the calibration curve, as shown in Fig. 4B. The fluorescence intensities of the BODIPY® 505/515 stained lipid were 246.8,
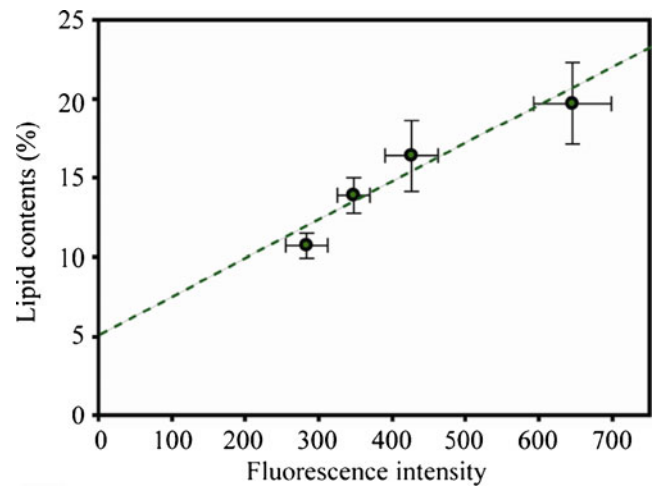

Fig. 5 Absolute quantitative analysis of the neutral lipids on the microfluidic device. Correlation of the fluorescence intensity of the BODIPY® 505/515 stained *C. reinhardtii* cells on the microfluidic device with the absolute lipid content measured by gas chromatography

324.3, 348.9, 371.8, 434.8, 447.4, 467.9, and 550.9 at the sodium acetate concentrations of 0, 1.43, 2.86, 4.29, 5.72, 7.15, 8.58, and 10.00 g L^{-1}, respectively (Fig. 4B). Thus, the corresponding lipid contents were calculated as 11.01, 12.81, 13.38, 13.91, 15.37, 15.67, 16.14, and 18.07 %, respectively. To our best knowledge, this is the first demonstration to correlate on-chip data with flask-scale data for the practical use of the high-throughput screening microfluidic device platform. Therefore, the fluorescence intensity obtained from the cultured BODIPY® 505/515 stained *C. reinhardtii* cells on a chip could be used for predicting the absolute lipid content of the cells that are cultured in the conventional flasks.

Conclusion

In this study, we have developed a high-throughput microfluidic device-based technique for screening microalgal cell culture conditions in an effort to obtain high growth rate and lipid content. The microfluidic device was designed by combining the concentration gradient channels and the cell culture chambers, so that the effect of the organic carbon source, sodium acetate in our model, on cell growth and lipid expression was explored. Statistical reproducibility of the growth and lipid analysis results was obtained by setting up eight different sodium acetate concentration gradients in a high-throughput manner and introducing five identical growth chambers onto each microchannel. The microfluidic experimental results were compared to the flask-scale experimental results to validate scalability. An absolute quantification method for analyzing the microalgal lipid content on the microfluidic device was established to enable the utilization of the screening microfluidic device platform for accelerating the process of the commercial production of biodiesel.

References

1. Chisti Y (2007) Biodiesel from microalgae. Biotechnol Adv 25(3): 294–306

2. Heredia-Arroyo T, Wei W, Hu B (2010) Oil accumulation via heterotrophic/mixotrophic *Chlorella protothecoides*. Appl Biochem Biotechnol 162(7):1978–1995. doi:10.1007/s12010-010-8974-4

3. Searchinger T, Heimlich R, Houghton RA, Dong F, Elobeid A, Fabiosa J, Tokgoz S, Hayes D, Yu T-H (2008) Use of U.S. croplands for biofuels increases greenhouse gases through emissions from land-use change. Science 319(5867):1238–1240. doi:10.1126/science.1151861

4. Pienkos PT, Darzins A (2009) The promise and challenges of microalgal-derived biofuels. Biofuels Bioprod Biorefin 3(4):431–440. doi:10.1002/bbb.159

5. Radakovits R, Jinkerson RE, Darzins A, Posewitz MC (2010) Genetic engineering of algae for enhanced biofuel production. Eukaryotic Cell 9(4):486–501. doi:10.1128/ec.00364-09

6. Wijffels RH, Barbosa MJ (2010) An outlook on microalgal biofuels. Science 329(5993):796–799. doi:10.1126/science.1189003

7. Cakmak T, Angun P, Demiray YE, Ozkan AD, Elibol Z, Tekinay T (2012) Differential effects of nitrogen and sulfur deprivation on growth and biodiesel feedstock production of *Chlamydomonas reinhardtii*. Biotechnol Bioeng 109(8):1947–1957. doi:10.1002/bit.24474

8. Li X, Xu H, Wu Q (2007) Large-scale biodiesel production from microalga *Chlorella protothecoides* through heterotrophic cultivation in bioreactors. Biotechnol Bioeng 98(4):764–771. doi:10.1002/bit.21489

9. Wang ZT, Ullrich N, Joo S, Waffenschmidt S, Goodenough U (2009) Algal lipid bodies: stress induction, purification, and biochemical characterization in wild-type and starchless *Chlamydomonas reinhardtii*. Eukaryotic Cell 8(12):1856–1868. doi:10.1128/ec.00272-09

10. Au S, Shih SC, Wheeler A (2011) Integrated microbioreactor for culture and analysis of bacteria, algae and yeast. Biomed Microdevices 13(1):41–50. doi:10.1007/s10544-010-9469-3

11. Hung PJ, Lee PJ, Sabounchi P, Aghdam N, Lin R, Lee LP (2005) A novel high aspect ratio microfluidic design to provide a stable and uniform microenvironment for cell growth in a high throughput mammalian cell culture array. Lab Chip 5(1):44–48

12. Lee PJ, Hung PJ, Rao VM, Lee LP (2006) Nanoliter scale microbioreactor array for quantitative cell biology. Biotechnol Bioeng 94(1):5–14. doi:10.1002/bit.20745

13. Hung PJ, Lee PJ, Sabounchi P, Lin R, Lee LP (2005) Continuous perfusion microfluidic cell culture array for high-throughput cell-based assays. Biotechnol Bioeng 89(1):1–8. doi:10.1002/bit.20289

14. Kim J, Taylor D, Agrawal N, Wang H, Kim H, Han A, Rege K, Jayaraman A (2012) A programmable microfluidic cell array for combinatorial drug screening. Lab Chip 12(10):1813–1822

15. Grunberger A, Paczia N, Probst C, Schendzielorz G, Eggeling L, Noack S, Wiechert W, Kohlheyer D (2012) A disposable picolitre bioreactor for cultivation and investigation of industrially relevant bacteria on the single cell level. Lab Chip 12(11):2060–2068

16. Dewan A, Kim J, McLean RH, Vanapalli SA, Karim MN (2012) Growth kinetics of microalgae in microfluidic static droplet arrays. Biotechnol Bioeng 109(12):2987–2996. doi:10.1002/bit.24568

17. Pan J, Stephenson AL, Kazamia E, Huck WTS, Dennis JS, Smith AG, Abell C (2011) Quantitative tracking of the growth of individual algal cells in microdroplet compartments. Integr Biol 3(10):1043–1051

18. Qu B, Eu Y-J, Jeong W-J, Kim D-P (2012) Droplet electroporation in microfluidics for efficient cell transformation with or without cell wall removal. Lab Chip 12(21):4483–4488

19. Holcomb R, Mason L, Reardon K, Cropek D, Henry C (2011) Culturing and investigation of stress-induced lipid accumulation in microalgae using a microfluidic device. Anal Bioanal Chem 400(1): 245–253. doi:10.1007/s00216-011-4710-3

20. Xia Y, Whitesides GM (1998) Soft lithography. Angew Chem Int Ed 37(5):550–575. doi:10.1002/(sici)1521-3773(19980316) 37:5<550::aid-anie550>3.0.co;2-g

21. Chen F (1996) High cell density culture of microalgae in heterotrophic growth. Trends Biotechnol 14(11):421–426. doi:10.1016/0167-7799(96)10060-3

22. Qiao H, Wang G (2009) Effect of carbon source on growth and lipid accumulation in *Chlorella sorokiniana* GXNN01. Chin J Ocean Limnol 27(4):762–768. doi:10.1007/s00343-009-9216-x

23. Siaut M, Cuine S, Cagnon C, Fessler B, Nguyen M, Carrier P, Beyly A, Beisson F, Triantaphylides C, Li-Beisson Y, Peltier G (2011) Oil accumulation in the model green alga *Chlamydomonas reinhardtii*: characterization, variability between common laboratory strains and relationship with starch reserves. BMC Biotechnol 11(1):7